THE HUMAN DENTATE GYRUS PLAYS A NECESSARY ROLE
IN DISCRIMINATING NEW MEMORIES

STEVENSON W. BAKER

A THESIS SUBMITTED TO
THE FACULTY OF GRADUATE STUDIES
IN PARTIAL FULFILLMENT OF THE REQUIREMENTS
FOR THE DEGREE OF
MASTER OF ARTS

GRADUATE PROGRAM IN PSYCHOLOGY
YORK UNIVERSITY
TORONTO, ONTARIO

July 2016

Abstract

Episodic memory provides us with the ability to re-experience unique events in rich detail. For this to occur, we must be able to 1) behaviorally "pattern separate" or discriminate new from old experiences, and 2) "pattern complete" or reinstate memories from partial cues. I report a rare individual with a specific lesion to the dentate gyrus of his hippocampus who has difficulty distinguishing between studied targets and unstudied lures that are visually similar. In addition, he displays a heightened tendency to recognize studied scenes from degraded pictures. These results provide the first direct evidence in humans that discriminating new memories cannot wholly function without an intact dentate gyrus and that this mnemonic ability is dissociable from, but likely interacts with, completion processes in the CA3 subfield of the hippocampus.

Acknowledgements

I wish to thank my supervisor, Dr. Shayna Rosenbaum, for her support and guidance and for helping me to grow as a researcher. I look forward to continuing to learn under her mentorship. I also thank Dr. Asaf Gilboa for his assistance in designing the experiment and valuable advice on data analysis and interpretation. Drs. Fuqiang Gao, Sandra Black, and Rosanna Olsen are thanked for assisting with anatomical analyses, and Dr. Thomas Wolbers and Paula Vieweg are thanked for helpful theoretical discussions. In addition, I am grateful for the participation of my thesis committee members, Dr. Jennifer Steeves, Dr. Gary Turner, and Dr. Doug Crawford for their time and advice. The Stark Memory Research Group at the University of California, Irvine and the Wolbers Aging and Cognition Research Group are acknowledged for permitting the use of stimuli developed in their labs. This Master's thesis was funded by Natural Sciences and Engineering Research Council (NSERC) Grant 04238-2014 to Shayna Rosenbaum. Finally, I am especially grateful to BL. This study would not have been possible without his participation.

Table of Contents

List of Tables

List of Figures

The Human Dentate Gyrus Plays a Necessary Role in Discriminating New Memories

Our day-to-day experiences are often highly similar to one another, occurring in the same place at the same time of day, with common people and objects, and with a shared purpose. Humans have an episodic memory to represent unique, personal events that are rich in detail (Tulving, 2000). For this to occur at least two basic neural mechanisms are required: one to discriminate or "separate" overlapping input patterns at encoding, and another to reinstate or "complete" memories from partial cues at retrieval (Hunsaker & Kesner, 2013; Marr, 1971; O'Reilly & McClelland, 1994; Rolls, 2016; Treves & Rolls, 1994). To what extent do these purported "pattern separation" and "pattern completion" mechanisms[1] rely on distinct subfields (e.g., dentate gyrus, CA3, CA1) of the hippocampus (Treves & Rolls, 1994)?

For over 40 years, psychologists and neuroscientists working with computational cognitive models have speculated that hippocampal networks support memories by creating non-overlapping neural representations at encoding that represent unique information about past events (e.g., Kesner & Rolls, 2015; Marr, 1971; McNaughton & Morris, 1987; Norman, Detre, & Polyn, 2008; O'Reilly & McClelland, 1994; Treves & Rolls, 1994; Rolls, 2016). Because of its role in learning (Rolls 2016), pattern separation is recognized as a fundamental component of episodic memory (Norman et al., 2008), a form of declarative memory for personally experienced events defined by their spatiotemporal context and recollection processes (Tulving,

---

[1] Throughout this paper, I use the terms pattern separation and pattern completion for ease of communication. However, this neuronal activity can only be inferred or approximated from the tasks described (e.g., Mnemonic Similarity Task and Memory Image Completion task). When used in regards to behavioural testing, PS and pattern completion should not be taken as synonymous with the neurophysiological processes involved in discriminating similar items, or in completing previous memories from partial cues. For more on this subject, see Leutgeb & Leutgeb (2014), Rolls (2016), Santoro (2013), and Schmidt et al. (2012).

2000). Pattern separation is often discussed in conjunction with the complementary process of pattern completion, or the recollection of a past experience or event from a degraded or incomplete cue (e.g., O'Reilly & McClelland, 1994; Rolls, 2016; Vieweg, Stangl, Howard, & Wolbers, 2015). Pattern completion is also essential to episodic memory, although it is believed to predominate during memory retrieval rather than at memory encoding (Hunsaker & Kesner, 2013; Norman et al., 2008). Indeed, the interplay between the two processes has led some to speculate that pattern separation and pattern completion are two ends of one larger, unitary operation, although this continuum concept is not without its critics (e.g., Hunsaker & Kesner, 2013). They point out that the two activities are clearly performed by different neuroanatomical structures and specialized computations during separable mnemonic phases (Treves & Rolls, 2004; Hunsaker & Kesner, 2013).

Neural Correlates of Pattern Separation/Pattern Completion

Lesion and genetic studies in rodents point to the dentate gyrus of the hippocampus as responsible for pattern separation and the CA3 subfield for pattern completion (Ahn & Lee, 2014; Gilbert, Kesner, & Lee, 2001; Kesner, Kirk, Yu, Polansky, & Musso, 2016; McHugh et al., 2007; Nakazawa et al., 2002; Neunuebel & Knierim, 2014). This classic dissociation is predicted by computational models (e.g., O'Reilly & McClelland, 1994; Rolls, 2016; Treves & Rolls, 1994), some of which provide a pattern completion/pattern association role for CA1 (Rolls, 2016; Tompary, Duncan, & Davachi, 2016), or a pattern separation-mediating role for the CA3 (Myers, & Scharfman, 2011).

However, the classic dissociation — which characterizes pattern separation in the dentate gyrus and pattern completion in the CA3 — is evolving with advancements in animal testing, higher-resolution neuroimaging and our knowledge of hippocampal neurogenesis, the birth of

new neurons. For example, there is recent rodent evidence of sparse coding throughout the hippocampus beyond dentate gyrus (e.g., Leutgeb, Leutgeb, Moser, & Moser, 2007; Deuker, Doeller, Fell, & Axmacher, 2014) and, conversely, a role for mature adult-born granule cells (GCs), which comprise a minor population of cells in the rat dentate gyrus, in pattern completion (e.g., Nakashiba, et al. 2012).

Human hippocampal formation: Dentate gyrus and CA3. Researchers attempting to verify computational models, or replicate animal studies, on the neural basis of pattern separation/pattern completion face various challenges in operationalizing these memory processes in healthy humans. One of the most daunting challenges is how to isolate the hippocampal network, or particular neural hubs thought to implement these cognitive abilities. In this regard, particular focus must be paid to three areas of the hippocampal formation and surrounding medial temporal lobe (MTL) cortices where pattern separation/pattern completion have been localized in rodent studies (e.g., Ahn & Lee, 2014; Neunuebel & Knierim, 2014): 1) the entorhinal cortex; 2) the dentate gyrus; and, 3) the CA3 subfield of the hippocampus proper. See Figure 1 (adapted from Duvernoy, 2005), for an illustration of the hippocampal formation, which includes the hippocampus proper (the cornu ammonis) — or the CA1, CA2, CA3 and CA4 subfields of the hippocampus — as well as the and the subiculum (Blumenfeld, 2010). (Within this paper, "hippocampus" will refer to the structures identified in this illustration of the hippocampal formation.)

Entorhinal cortex and trisynaptic loop. Although human studies of pattern separation typically involve visual stimuli, particularly those that are spatial in nature (in recognition of the importance of visuospatial context to episodic memory; Rolls, 2016), pattern separation/pattern completion models allow for discrimination of any perceptual input to the dentate gyrus

(Hunsaker & Kesner, 2013). For example, Weeden, Hu, Ho and Kesner (2014) found that efficient pattern separation for odors in rats was dependent on the ventral dentate gyrus.

Whatever the input, the pattern separation process begins with the entorhinal cortex. It is the main interface between the MTL (parahippocampal cortex, perirhinal cortex, hippocampus) and the higher-order association cortices of the brain. The entorhinal cortex acts as a relay for neural activity from the neocortex before that activity is projected onto the archicortex, or the three-layered cell structure of the hippocampus (Marr, 1971).

The perforant pathway, so called because it crosses, or "perforates," the subiculum (Witter, 2007), is the main entorhinal cortex efferent to the hippocampus. The most studied destination of this pathway (and one discovered by Ramón y Cajal) is the dentate gyrus (Witter, 2007). Lesser-studied projections also travel from the entorhinal cortex to the CA1 and CA3 (Blumenfeld, 2010; Rolls, 2016; Witter, 2007). Furthermore, and essential to our understanding of pattern separation, the pyramidal cells of the CA3 receive inputs from the dentate gyrus via unmyelinated axons known as the mossy fiber pathway (O'Reilly & McClelland, 1994, Rolls, 2016). CA3 neurons project onto the CA1 and neural signals from there feedforward to the entorhinal cortex. In addition, CA3 neurons synapse onto other CA3 cell bodies through "recurrent collaterals" (Rolls, 2016). This "entorhinal cortex → dentate gyrus → CA3 [↔ CA3] → CA1 → entorhinal cortex" network is sometimes referred to as the trisynaptic circuit or loop (Blumenfeld, 2010). A schematic of the circuit is provided in Figure 2 (from Rolls, 2016), with forward connections throughout the hippocampus noted in solid lines and backprojections to the neocortex illustrated in dashed lines.

Pattern separation within the hippocampus. To probe the process of hippocampal pattern separation in greater detail, we can start by examining the co-occurring neocortical

elements of a new episode (e.g., the spatiotemporal contexts of a new memory) and how they are separated within the hippocampus via processing stages or neural pathways.

First, the neocortical elements arrive at the entorhinal cortex from the higher-order association areas of the brain. From layer 2 of the entorhinal cortex, the inputs are transmitted across the perforant pathway to the dentate gyrus and the CA3 (Witter, 2007; Leranth & Hajszan, 2007, Rolls, 2016). As the granule cells of the dentate gyrus have approximately five times as many neurons as the entorhinal cortex (one million versus 200,000 in rodents; Newman & Hasselmo, 2014), the dentate gyrus is able to separate the efferents from the entorhinal cortex across a more widely distributed, or "sparse" (in terms of neural representations) network (Norman et al., 2008; O'Reilly & McClelland, 1994). These distributed and orthogonal episodic representations are then projected onto the CA3 via the mossy fiber pathway (Norman et al., 2008; O'Reilly & McClelland, 1994; Rolls, 2016). In rats, the connections from the dentate gyrus to the CA3 are "sparse but possibly powerful . . . each CA3 cell receives approximately 46 mossy fiber inputs" (Rolls, 2016, p. 6). In effect, then, the dentate gyrus widens the elements of the signal from the entorhinal cortex, so that small signal changes in the entorhinal cortex lead to much larger ones in the dentate gyrus, resulting in more distinct and non-overlapping patterns of activation (Leutgeb, Leutgeb, Moser & Moser, 2007; Norman et al., 2008; Newman & Hasselmo, 2014). The amplified detail is then transmitted from the dentate gyrus to the CA3 in a narrower, widely distributed band, where it is stored in slightly larger clusters of neurons, which can be later triggered by retrieval cues for the pattern (Norman et al., 2008; Rolls, 2016).

As noted above, the trisynaptic connections from the CA3 back to the entorhinal cortex ensure that pattern-separated memories have an integrative link from the archicortex to the neocortex (Leranth & Hajszan, 2007; Rolls, 2016). In addition, the recurrent collaterals within

the CA3 serve to bind together the different elements of the pattern-separated event and allow for more successful pattern completion from partial cues, as even a fragment of the pattern can activate the entire interconnected CA3 learning episode (Knowlton & Eldridge, 2006). As the title of one paper (Newman & Hasselmo, 2014) on the subject summarized pattern separation/pattern completion, "CA3 sees the big picture while dentate gyrus splits hairs." See Figure 3 (from Rolls, 2016) for an illustration of the relative inputs onto each CA3 rat cell from the performant pathway, mossy fiber, and recurrent collaterals (connections from one CA3 axon onto another CA3 dendrite).

Human Evidence for Pattern Separation

Our understanding of the neural substrates of pattern separation in humans can be inferred from functional neuroimaging, neuropsychological testing correlated with structural neuroimaging, and case studies of individuals with hippocampal lesions. Breakthroughs in high-resolution functional magnetic resonance imaging (fMRI), in particular, have enabled localization of brain activity to hippocampal subfields, although it has been difficult to functionally separate the dentate gyrus and CA3 subfields with currently available methodologies (Lacy, Yassa, Stark, Muftuler, & Stark, 2011). However, behavioral tasks designed to approximate pattern separation and pattern completion have been shown to elicit the predicted pattern of activity in dentate gyrus and CA3/CA1 (Bakker, Kirwan, Miller, & Stark, 2008; Chadwick, Bonnici, & Maguire, 2014; Lacy, Yassa, Stark, Muftuler, & Stark, 2011; Tompary, Duncan, & Davachi, 2016). Indeed, Bakker et al. (2008) used 3 Tesla (T) fMRI to scan healthy participants as they performed a modified recognition memory test. This test required participants to discriminate between highly similar images of everyday objects. During discrimination, participants' dentate gyrus/CA3 was more active than other subregions of the

hippocampus. Although the authors acknowledged that the high-resolution MRI used was not sufficient to distinguish between the CA3/dentate gyrus, they speculated that since the discriminated activity patterns of the dentate gyrus are projected onto the CA3 via the mossy fiber pathway, even higher resolution scanning would have yielded similar results (Bakker et al., 2008). Partially supporting this claim are the findings from the neuroimaging, brain volume analyses and behavioural testing conducted by Doxey and Kirwan (2015). They discovered that precision in pattern separation in older and younger participants correlated with brain volumes in left dentate gyrus and CA3, more than it did in other hippocampal sub-fields or MTL sub-regions.

The Present Case Study

While encouraging, the human evidence described above yields data that are indirect and correlational, and lacks the precision to distinguish between the dentate gyrus and CA3. Examination of discrimination and completion processes in individuals with selective lesions to hippocampal subfields is needed to infer causation in humans (Chadwick et al., 2014). Reports of discrimination deficits in patients with hippocampal lesions exist (Duff et al., 2012; Kirwan et al., 2012), but the lesions in these cases likely encompass other subfields and, in many cases, extend beyond the hippocampus into adjacent MTL regions. To my knowledge, pattern completion has not yet been tested in patients with hippocampal lesions. Moreover, very few cases with damage restricted to a specific subfield of the hippocampus have been documented in the literature and, in the even fewer cases that correlated findings from neuropsychological testing with postmortem neuropathological examinations, it is the CA1 subfield that is compromised (Rempel-Clower, Zola, Squire, & Amaral, 1996; Zola-Morgan, Squire, & Amaral, 1986).

In the current thesis, I report the rare case of BL, a 54-year-old man who experienced electrical injury and cardiac arrest over 20 years ago. This event resulted in highly selective bilateral ischemic lesions to the dentate gyrus that partially extend into CA3 (Figure 4, Figure 5); other regions implicated in pattern separation and pattern completion, including entorhinal and perirhinal cortices, appear to have been unaffected. Studying BL provides the unique opportunity to directly evaluate, for the first time, theories of hippocampal function that assign the dentate gyrus a specific role in discriminating old from new memories.

Hypotheses. Given the lesion in BL's dentate gyrus, the network architecture of the hippocampus, as well as evidence that older adults with age-related volume hippocampal loss perform more poorly on pattern separation tasks (Stark et al., 2013), I hypothesize that BL will be impaired relative to age-matched, healthy controls in his ability to discriminate memories. His general recognition memory will be intact, but his ability to identify similar looking visual items (i.e., lures) on an established pattern separation task (Stark et al., 2013), will be deficient.

In addition, if speculation that pattern completion relies upon the distinction of partially overlapping sensory experiences, and, as this separation output from the dentate gyrus projects onto the CA3, I also predict that BL will show a similar inclination towards overactive episodic completion of memories, as measured by a novel task of pattern completion (Vieweg et al., 2015). In this way, discrimination and completion are recognized as complementary processes, requiring a fine balance between establishing and dissociating new memories, and reconstructing old ones. For example, models of aging propose that strengthening of the CA3 autoassociative function leads to the over-expression of old information at the expense of discriminating new information (Wilson, Gallagher, Eichenbaum, & Tanila, 2006). Behavioral evidence for a bias toward completion in older adults was recently demonstrated in age-related recognition

differences between learned and new items (Vieweg et al., 2015). Because of this discrimination/completion interplay, and because output from the DG projects onto CA3 (Rolls, 2016; Bakker et al., 2008), I predict that BL will show an inclination to recall scenes already learned when presented with incomplete new pictures.

Method

Participants

Patient BL. The current case study focused on BL, a 54-year-old man with 13 years of education. In 1985, he was diagnosed with hypoxic-ischemic brain injury following an electrical injury and cardiac arrest (Kwan et al., 2015). Standard neuropsychological testing (Table 2) revealed mildly impaired anterograde memory and moderately impaired retrograde episodic memory, which improved when BL was given specific personal cues (Kwan et al., 2015). The only other area of relative weakness was within the visuospatial domain on the copy condition of the Rey-Osterrieth Complex Figure, which may relate to volume loss within superior-posterior parietal cortex (see Table 1). It is unlikely that this deficit and volume loss explain performance on tests of pattern separation and completion. Moreover, regions of inferotemporal cortex known to be involved in object recognition remain structurally intact. Recent high-resolution 3T MRI scans of BL's hippocampus revealed selective bilateral ischemic lesions that are limited to the dentate gyrus and a portion of CA3 (Figure 4, Figure 5). Other regions implicated in pattern separation and pattern completion, including entorhinal and perirhinal cortices, appear to have been unaffected (Table 1).

MRI acquisition. Structural MRI images were acquired using a 3T Siemens Trio scanner at Baycrest to examine the effects of global hypoxia/ischemia on BL's hippocampus (including subfields). A whole-brain T1-weighted MPRAGE sequence (TE/TR = 2.63 ms/2000 ms, 176

oblique axial slices, 256x192 matrix, voxel size = 1x1x1 mm, FOV = 256 mm) was acquired to obtain a measure of total brain volume and for confirmation of anatomical boundaries best viewed in the sagittal and/or axial plane. For later segmentation, a second high-resolution T2-weighted structural image (HRH-T2) was acquired in an oblique coronal plane, perpendicular to the long axis of the hippocampus (TE/TR = 68 ms/3000, 22-28 slices, 512x512 matrix, voxel size of 0.43x0.43x3 mm, no skip, FOV=220mm), along with fluid-attenuated inversion recovery (FLAIR).

Hippocampal segmentation. Signal abnormalities were examined on FLAIR and HRH-T2; no signal abnormalities were noted in the CA1-2 and subiculum, cerebral cortex, and subcortical nuclei. However, on the coronal HRH-T2 inverted images (see Figure 5) BL showed a unique pattern in his hippocampal lesion, with hyperintensities limited to the dentate gyrus bilaterally (from the head to tail). In addition, hippocampal lesions — limited to almost the entire dentate gyrus bilaterally — were evident on the sagittal HRH-T2 inverted images (Figure 5C).

Volumetric quantification of the hippocampal subfields was then performed on the HRH-T2 of BL using Analyze 12.0 software and compared to the 119 age-matched controls examined by Mueller and Weiner (2009). An additional three age-matched controls were scanned on the same 3T scanner using the same neuroimaging protocol as BL for validation purposes. Subsequent manual segmentation of the hippocampal subfields of BL and controls aligned with the published procedure (Mueller & Weiner, 2009). The steps are noted in the following paragraph.

External and internal hippocampal landmarks were used as markers to delineate the following subfields: CA1, CA1-2 transition zone, CA3/dentate gyrus (combined as one section) and subiculum. Subdivision into these sections started with the first slice of the hippocampus on

which the hippocampus head was no longer visible. The hippocampal subfields noted above were drawn manually on this cut, as well as on the following slice (6 mm range overall). Following this demarcation, segmentation proper began with a delineation of the CA1/subiculum. In order to determine this border, a line was drawn at right angles from the edge of subiculum to the medial border of the hippocampus. Next, a region assumed to be CA2 was marked as a tiny (tiny relative to the other subfields) square; its height at the CA1/CA2 boundary also determined its length. In addition, the overall shape of the CA2 was established by the outer boundary of the hippocampus and the hypointense myelinated tissue in the stratum radiatum/lacunosum-moleculare (SRLM). Adherence to recommendations from the protocol (Mueller & Weiner, 2009) was used to name the CA2 squared region the CA1-2 transition zone. Moving medially and ventrally from there, the remainder of the hippocampus — CA3 and dentate gyrus — was grouped as one region (i.e., CA3+dentate gyrus). Although only higher resolution MRI (e.g., 7 Tesla) can currently distinguish between dentate gyrus and CA3 in living humans, the manual segmentation of dentate gyrus and CA3, when combined with visual inspection of the T2 inverted images, led to speculation that the majority of BL's volume loss resides in the core of his hippocampus, i.e., within BL's dentate gyrus. A visual representation of the segmentation of the hippocampal subfields of BL and a control can be found in Figure 4.

Volumetric analysis (MTL). Volumetric analysis of BL's hippocampus and surrounding MTL cortices indicated that his dentate gyrus is nearly 50% smaller (whereas CA1 is 8% larger) than in 119 age-matched controls (Mueller & Weiner, 2009). Although current hippocampal segmentation protocols have difficulties distinguishing dentate gyrus from CA3 (Bakker et al.; Kirwan et al., 2008; Yushkevich et al., 2015), when considered together with the inverted T2-

weighted images, it is clear that the majority of the volume loss sustained in BL is within his dentate gyrus (Figure 4, Figure 5) and did not affect entorhinal or perirhinal cortices.

Whole-brain analysis. In order to probe potential cerebral atrophy in select regions of interest throughout the brain, T1-weighted MRI images for BL and 8 age-matched controls were converted to MGZ files that were then used by FreeSurfer for cortical reconstruction via a chain of automated scripts. The reconstruction scripts automatically performed anatomical conformation, intensity normalization, skull stripping, subcortical segmentation and labelling, surface reconstruction and (spherical) registration, cortical parcellation, and generation of statistics files containing measurements including volume, area, and thickness. Following the completion of the automated reconstruction, the 2D volume slices and 3D surfaces were visually inspected using FreeSurfer's tkmedit and tksurfer, and no notable abnormalities were found. Nine regions of interest generated by cortical parcellations in FreeSurfer were then normalized by estimated intracranial volume (eTIV) for BL and controls. Volumes of key brain regions known to be involved in visuospatial construction and object recognition are presented in Table 1.

Control participants. BL's performance was compared to that of 20 healthy, right-handed control participants in Experiment 1 (mean age = 52; mean education = 14 years; 10 males) and 19 healthy, right-handed control participants (mean age = 51; mean education = 14 years; 13 males) in Experiment 2. Thirteen controls were common to both experiments (mean age = 51; mean education = 14.5 years; 9 males). Comparisons of hippocampal subfield volumes in BL with published data from 119 age-matched controls (Mueller & Weiner, 2009) based on a manual segmentation protocol was validated in 3 additional male participants (mean age = 53; mean education = 15.6 years) who underwent high-resolution structural MRI. Separate whole-

brain analysis was conducted in BL in comparison to 8 additional participants (mean age = 51.3; mean education = 14.8 years; 3 males).

Controls had no history of psychiatric or neurological illness. They were recruited through the Baycrest Health Sciences participant pool and by word of mouth and were reimbursed $15/hour according to the suggested rate at Baycrest. Informed consent was obtained in accordance with the Ethics Review Boards at York University and Baycrest, and conforms to the standards of the Canadian Tri-Council Research Ethics guidelines.

Procedure: Experiment 1

The goal of Experiment 1 was to evaluate BL's behavioural discrimination abilities (Stark et al., 2013) relative to that of a control group on a task that approximates pattern separation. In order to evaluate these abilities, BL and controls were tested on the Mnemonic Similarity Task (MST; Stark, Stevenson, Wu, Rutledge, & Stark, 2015), formerly known as the Behavioral Pattern Separation Task (BPS-O; Stark et al., 2013). The MST assesses recognition memory performance using a paradigm similar to that used to test patients with hippocampal lesions (Kirwan et al., 2012) and conceptually similar to a visual recognition task used with rodents (Ahn & Lee, 2014). The MST was administered as a stand-alone application on a laptop running Windows 7. Participants were randomly assigned one of two MST stimulus sets (set "C" or "D"). BL was tested twice (three weeks apart between testing), once on each version, and with similar bias metric scores (3.0 and -2.13, respectively) in both sessions. Administration of the MST followed a published protocol (Stark et al., 2013). The steps are described below.

Study phase: During the study phase, participants viewed 128 color images of everyday objects (e.g., picnic basket, fishbowl, saxophone), each for 2 s, followed by a 0.5 s interstimulus

interval (ISI). For each image, participants judged via button press whether the object depicted was primarily an outdoor item or indoor item. (See Figure 6.)

Test phase: Following the study phase, participants were administered a surprise recognition memory test. During this test, they were randomly presented with 192 images, each onscreen for 2 s, followed by a 0.5 s ISI. The images at test included 64 targets (i.e., studied objects), 64 foils (unrelated and unstudied images), and 64 lures (objects conceptually and perceptually similar to the studied items) (Figure 6). Participants were asked to classify with a button press whether each image presented was *old*, *new*, or *similar* to the items presented at study.

Performance on the MST was evaluated through the Lure Discrimination Index (LDI) score (Stark et al., 2015), which is thought to provide a sensitive measure of pattern separation (Stark et al., 2013). The LDI score for each participant was computed as the difference between the rate of "Similar" responses given to lure stimuli minus the rate of "Similar" responses given to foil items (Stark et al., 2015). This value was then averaged across participants, thus gauging the overall ability of the group to pattern separate, while at the same time correcting for potential response biases of participants when faced with unlearned items (Stark et al., 2013; Stark et al., 2015).

Procedure: Experiment 2

The goal of Experiment 2 was to assess BL's pattern completion tendencies relative to a control group. To do so, the recognition memory abilities of BL and controls were tested with a novel task, which has recently been named the Memory Image Completion (MIC) task by the test designers (Vieweg, et al., 2015). The MIC was administered as a stand-alone MATLAB

application on a laptop running Windows 7. This experiment followed the procedures for the MIC described in Vieweg et al. (2015), as described below.

*Study phase***:** During the study phase, participants viewed images of each exemplar for 2 s. Every image was preceded by a title screen, which identified the exemplar by name (bar, bedroom, dining room; kitchen, library; see Figure 7). Each of the five studied scenes, together with five novel items, was then randomly presented for 2 s. After viewing each image, participants were asked to indicate if the scene was studied or if it was new, and, if applicable, which scene it was specifically. After correct identification of each learned stimulus in three consecutive trials, participants could proceed to the test phase.

Test phase: During this phase of the experiment, the five original exemplars (bar, bedroom, dining room; kitchen, library) were randomly presented, intermixed with five novel scene items. Both the studied and novel items were presented in complete (100% completeness) or masked (i.e., degraded) form (35%, 21%, 12%, or 5% completeness), resulting in 50 test items. Each item was presented four times (resulting in 100 old and 100 new images) for 2 s. Two forced choice tasks — stimulus identification and confidence rating — followed presentation of studied and novel items. Responses were self-paced and included these following choices for each trial: *bar*, *bedroom*, *dining room*, *kitchen*, *library*, *none of these* (the latter indicating that the stimulus was new).

Performance on the MIC was evaluated through MIC bias scores, calculated as the difference in accuracy scores for learned minus new stimuli for each participant and for each level of stimulus completeness. Higher bias scores, therefore, are indicative of relative weakness in identifying new stimuli and point to an elevated tendency toward pattern completion.

Results

In a first experiment, I tested BL's behavioural discrimination abilities on the Mnemonic Similarity Task (MST; Stark et al., 2013), which evaluates recognition memory performance using images of everyday objects. As in traditional recognition memory experiments, other visual images at test include a subset of the studied objects (i.e., old items or "targets"), intermixed with unrelated "foils" (i.e., new items). In addition, they include "lures," a special kind of unstudied foil that is similar to the target items in terms of appearance and conceptual category. During the test phase of the MST, participants had to classify each of the 192 images viewed as old, new, or similar.

I hypothesized that, like controls, BL would be able to identify targets and foils, even though standard neuropsychological testing of BL revealed mildly impaired anterograde memory and moderately impaired retrograde memory (Kwan et al., 2015; see Table 2). Given that the volume reduction in BL's hippocampi largely occurred within the dentate gyrus, I further hypothesized that he would be impaired relative to controls in his ability to identify lures. These predictions are based on evidence that the MST is sensitive to declines in encoding and discriminating similar items experienced by healthy older adults and individuals diagnosed with amnestic mild cognitive impairment (Stark et al., 2013, 2015).

To ensure reliability of findings in a single case, BL was tested on two versions of the MST, and his performance was compared to controls' using Crawford and Howell's modified *t*-test for single cases (Crawford & Garthwaite, 2002). This test treats the control sample's data as statistics, rather than as parameters, controlling for Type I errors when testing whether a single case's score is significantly below that of controls (Crawford & Garthwaite, 2002). It also provides estimates of the percentage of the normal population falling below a single case's score

Crawford, Garthwaite, & Slick, 2009), as well as the confidence interval (CI) on the observed result. BL's performance was similar to that of controls in correctly identifying targets, $t(19) = -0.24$, $p = .82$, which would place him at the 41st percentile, 95% CI [25, 58], and identifying foils, $t(19) = -0.98$, $p = .34$, which would place him at the 17th percentile, 95% CI [6, 32]. However, BL performed significantly worse than controls in identifying lures; $t(19) = -2.50$, $p = .02$, which would place him at the 1.1 percentile, 95% CI [0.03, 5.14]. See Figure 8. He incorrectly identified lures as old nearly five times more often than he correctly identified them as similar. This pattern of findings is further emphasized by BL's LDI score (Stark et al., 2015), which, again, is calculated as the difference between the rate of "similar" responses given to lure items and "similar" responses given to foils, to determine the presence of a response bias. BL's LDI score was close to zero, reflecting a selective insensitivity to lures that was not apparent in controls ($t = -2.18$, $p = .04$), placing him at the 2.1 percentile, 95% CI [0.11, 8.19].

In a second experiment, I tested BL on the Memory Image Completion (MIC) task (Vieweg et al., 2015), which evaluates recognition memory performance with 10 black and white line drawings of indoor scenes (Hollingworth & Henderson, 1998). Half of the scenes are learned at study (targets) and randomly presented at test with five new scenes (foils). Importantly, the five targets and five foils are presented four times each, masked in five different degrees of completeness (100%, 35%, 21%, 12%, 5%). The tendency of participants to mentally complete the images is gauged by their bias toward identifying the foils as targets.

BL's ability to correctly identify the targets, or learned items, was highly similar to that of controls, particularly at the 100%, 35% and 21% levels of stimulus completeness. A dramatic difference in performance was seen, however, in BL's responses to the foils. Overall, he was able to identify only 28% of the foils as new, compared to 79% of foils identified by controls,

representing a significant difference; $t(18) = -2.92, p = .01$ (Figure 9). It is notable that 30 healthy older adults tested in a separate study identified 55% of foils (Vieweg et al., 2015). Bias scores — calculated as the difference in accuracy scores for learned minus new stimuli for each participant and for each level of stimulus completeness — were also significantly greater for BL than for controls (Figure 10).

Indeed, when presented with a foil, BL was 2.5 times more likely to erroneously confuse the new image with a learned one. BL showed this bias ($p < .05$) at every level of stimulus completeness. The MIC also illuminates BL's deficit in discrimination; his 30% false alarm rate for new images that were unmasked (i.e., presented at 100% completeness) suggests a failure to pattern separate. Still, the difference between BL's bias scores of the degraded images (averaged across levels of completeness) and his score for the 100% presentation rate was significantly higher ($p = .03$) relative to this same difference in the 13 controls tested on both the MST and the MIC, indicating that his exaggerated pattern completion tendency was over and above his impaired pattern separation. The difference between the two tasks can be further examined by contrasting BL's average bias scores for the MST via the LDI with the average bias score for the degraded images of the MIC (relative to the same comparison in controls; see Figure 10). The Revised Standardized Difference Test (Crawford & Garthwaite, 2005) revealed a significant difference between BL and controls on the two tasks, $t(12) = 4.31, p = .001$, indicating a differential deficit (Crawford & Garthwaite, 2005).

Importantly, as would be expected with an apparent pattern separation deficit and an overexpression of pattern completion, false alarm responses on the MIC were not random. BL's first false alarm choice exceeded all other false alarms by a wide margin (100%), emphasizing that when he erred, he was predisposed to complete towards the learned stimulus that was most

similar to the new image perceptually and conceptually. For example, BL correctly identified the office (new image) as new the four times it was presented at 100% completion. Every time the office image was presented in a masked version, however, he made a false alarm, with 13 out of 16 (81%) of the false alarms completed to the studied image of the library (see Figure 9A for images of the library and the office).

Discussion

In an individual with selective lesions to the dentate gyrus, behavioural discrimination is specifically impaired. This deficiency is paired with a bias towards image completion, suggesting that what remains of the CA3 is functional and receives input from the entorhinal cortex via the perforant pathway (Rolls, 2016). If BL's lesion did render the CA3 dysfunctional, it might be taken to suggest that the CA3 does not play a critical role in discrimination of similar memories or in memory cue completion. Alternatively, other regions might compensate for possible CA3 dysfunction, such as an intact CA1 (Lacy et al., 2011; Tompary et al., 2016), which interacts with CA3 and extra-hippocampal cortices in reinstating complete memories from partial cues (Rolls, 2016; Tompary et al., 2016). Interestingly, the CA1 subfield of BL's hippocampus is slightly larger than average.

Meanwhile, BL's other recognition memory abilities — his capacity to correctly identify the MST/MIC targets as old and the MST foils as new — are similar to controls. It can thus be concluded that BL displays a selective deficit in behavioral discrimination that coincides with hippocampal damage limited to the dentate gyrus. Until now, few cases with damage restricted to a specific subfield of the hippocampus have been documented in the literature, and in those cases, it is the CA1 that is compromised (Rempel-Clower et al., 1996; Zola-Morgan et al., 1986). Moreover, to my knowledge, pattern completion has not been tested in patients with

hippocampal lesions. The current results lend validity to cross-species studies and less direct methods of investigating dentate gyrus contributions to pattern separation in humans, including computational models and high-resolution fMRI (Berron et al., 2016; Rosenbaum, Gilboa, & Moscovitch, 2014).

The current lesion data might also inform the debate on process interplay, and may be applied to the question of whether pattern separation and pattern completion are two sides of the same coin or opposite ends of a continuum (Hunsaker & Kesner, 2013; Molitor, Ko, Hussey, & Ally, 2014; Vieweg et al., 2015; Yassa et al., 2011). A key element of this debate — as with other topics in cognitive neuroscience — concerns the process purity of the behavioral paradigms used to assess these cognitive operations (e.g., Molitor et al., 2014). In the current study, even though it is assumed that the MST and MIC approximate pattern separation and pattern completion, respectively, there are other neural computations, both upstream and downstream from the dentate gyrus, which can help differentiate new information from preexisting memory traces (Deuker et al., 2014; Leutgeb et al., 2007; Myers, & Scharfman, 2011). One key to our understanding of sparse coding and memory completion may lie in cross-species studies of hippocampal neurogenesis and the way in which adult-born dentate gyrus granule cells mediate pattern separation/pattern completion processes (Danielson et al., 2016; Johnston, Shtrahman, Parylak, Gonçalves, & Gage, 2016; Nakashiba, et al. 2012). Other avenues of investigation will include the recurrent collateral connections within CA3, which, through neural backprojections, can exert an inhibitory influence upon dentate gyrus granule cells, facilitating dentate gyrus-to-CA3 pattern separation (Myers & Scharfman, 2011).

Limitations and Future Directions

One limitation of this case study is that it tests pattern separation and pattern completion using stimuli from one modality (i.e., visual). This is not unusual, as human studies of pattern separation/pattern completion typically use visual object information (e.g., Bakker et al., 2008; Kirwan et al., 2012; Tompary et al., 2016); animal studies also tend to use visual or visuospatial information (e.g., Ahn & Lee, 2014; Leutgeb et al., 2007). However, it does pose the question of whether the mnemonic phenomena being studied are specific to the visual domain. However, even within the visual domain, the MST uses pictures of objects and the MIC uses pictures of scenes, which are dissociable in terms of where they are processed in the brain. A large body of research has shown that the ventral visual-processing stream is primarily involved in processing the identity of an object (i.e., "what"), whereas the dorsal visual-processing stream is primarily involved in processing the location of an object ("where"; Ungerleider & Mishkin, 1982; Ungerleider & Pasternak, 2004). The dorsal and ventral streams project to the parahippocampal and perirhinal cortices, respectively (Suzuki & Amaral, 1994). The visuospatial information projects from the parahippocampal cortex to the medial entorhinal cortex, whereas the object information travels from the perirhinal cortex to the lateral entorhinal cortex (Rolls, 2016; Leutgeb & Leutgeb, 2014). Thus, it is possible that the MST and MIC are probing not only distinctions in discrimination and completion, but also dissociations in diverse perceptual input, managed within different visual pathways/systems (e.g., Barense, Henson, Lee, & Graham, 2010). However, there is evidence that object and visuospatial information — as well as all other sensory modality input — travels from layer two of the entorhinal cortex along the perforant pathway to converge upon the dentate gyrus and the CA3 subfield (Rolls, 2016). Whether the brain is presented with pictures of objects (Stark et al., 2013) or scenes (Vieweg et al., 2015), or

even various odors (Weeden Hu, Ho, and Kesner, 2014), the ability to discriminate between interference caused by similar and competing inputs would still, theoretically, tax the same areas of the dentate gyrus and CA3, regardless of the degree to which that information is already discriminated in sensory and perceptual areas upstream from the entorhinal cortex.

Still, the use of visual stimuli with pre-experimental associations — for example, stimuli which can be semantically identified (e.g., a tricycle) — could point to other confounds: that is whether the conceptual knowledge of the item leads participants to mentally produce a linguistic semantic association when mentally processing the object (e.g., "trike"), or an episodic autobiographical association (e.g., "that looks like the trike I received for my fourth birthday"). These semantic/episodic "tags" (Hunsaker & Kesner, 2013) could influence pattern separation/pattern completion performance and compromise the validity of the experimental paradigm (Hunsaker & Kesner, 2013; Liu, Gould, Coulson, Ward, & Howard, 2016).

The fact that rodents, which presumably do not have similar language regions or episodic memories as people, also show pattern separation/pattern completion dissociations for visual stimuli, could lessen the impact of this accusation (Hunsaker & Kesner, 2013). Future research in this area, however, would benefit from using stimuli devoid of pre-experimental semantic or episodic associations. Indeed specialists in this area are now calling for the use of "abstract, never-before-seen-objects" (Liu et al., 2016, p. 706) as a way of improving the validly of tasks to assess pattern separation/pattern completion in healthy humans. In response to this call, future testing planned for BL includes using stimuli in other modalities (e.g., sounds) or using visual stimuli lacking in semantic salience (e.g., abstract images).

Through continued work with BL, we plan to build on his case study and further enhance understanding of the basis of hippocampal contributions to episodic memory. A greater

understanding of pattern separation and pattern completion processes afforded by such work will do more than just increase our theoretical knowledge of the functional architecture of the human hippocampus. It will also help to move forward the implementation of clinical assessments and interventions based upon the relationship between the aging brain and pattern separation/completion deficits (Gilbert, Holden, Sheppard, & Morris, 2016). Hippocampal dentate gyrus/CA3 hyperactivity (and bias to pattern completion), in particular, is now being studied as a modifiable biomarker for such disorders as Alzheimer's disease and dementia (M. Yassa, personal communication, July 25, 2016). And gaining a better understanding of how the dentate gyrus/CA3 might overgeneralize episodic details relating to threat and fear might help guide the development of novel therapeutic strategies for posttraumatic stress disorder (Besnard, & Sahay, 2016; Wang et al., 2010).

A final limitation of the study is shared by all case studies which attempt to infer brain-mind relationships from one individual, or from one lesion. Although single case studies of individuals with hippocampal damage have been invaluable in defining the neural architecture of the medial temporal lobes and in confirming hypotheses about hippocampal involvement in episodic and semantic memory (Rosenbaum et al., 2014), they have inherent limitations. In some cases, group designs may be superior at assembling converging human and animal evidence in testing complex predictions of basic cognitive processing systems (Robertson, Knight, Rafal, & Shimamura 1993). In addition, in the present case I have investigated an individual who may have a lesion overlapping two hippocampal subfields (dentate gyrus and CA3). Until confirmatory evidence can be found (e.g., through 7 Tesla neuroimaging), I can only use the currently available best methods and consult with the best specialists to determine that BL's

lesion is primarily within his dentate gyrus, and infer how this damage leads his discrimination and completion biases.

A strong inferential point in favour of the speculation that the majority of BL's CA3 is intact is his ability to retrieve memories of studied items, performing similar to controls in recognition of target items in both MST and MIC tests. If the CA3 were also lesioned, it is unlikely that he would be able to retrieve episodic memories (e.g., Chadwick, Bonnici, & Maguire, 2014; Newman & Hasselmo, 2014; Rolls, 2016) and thus would be significantly impaired relative to controls on recognition memory tests. This observation is further supported by animal evidence of CA3 being crucial to associative memory recall (Farovik, Dupont, & Eichenbaum, 2010; Nakazawa et al., 2002).

Since BL's lesion occurred in 1985, a further avenue of exploration might be how his hippocampus has adapted to this lesion over the decades. Maguire and colleagues (2000), in their study of London taxi drivers, were able to show that the cabbies had significantly lager posterior hippocampi than controls. The conclusion drawn was that the experienced London taxi drivers exhibited pronounced enlargement, brain *plasticity*, in regards to years of driving the labyrinthine routes of London. Could BL also exhibit such plasticity in response to dentate gyrus/CA3 damage, for example, through his larger than normal CA1? A recent study of healthy adults using high-resolution fMRI and multi-voxel pattern similarity analyses (Tompary et al., 2016) found that successful episodic recollection is correlated with pattern reinstatement in the CA1 (and the perirhinal cortex). Testing BL on a similar paradigm might confirm or expand upon these findings about the involvement in pattern discrimination/reinstatement of other subfields within the trisynaptic circuit.

Concluding Remarks

        Taken together, the evidence offered within this paper suggests that BL presents with selective deficits in assigning less overlapping, more independent neural codes to similar items. This finding suggests that pattern separation and pattern completion processes influence each other but are dissociable as approximated by the MST and the MIC. I speculate that BL's dentate gyrus cannot process and project sparse information onto his CA3, or that his CA3, similar to that of rats exploring changed environments, can only decorrelate relatively substantial differences between inputs (Deuker et al., 2014; Leutgeb et al., 2007). The result is that details about past events exist, but they are more coarsely represented, so that when BL sees a fragment of any visual stimulus, he is more likely to confuse it with a previously experienced item than to recognize it as being new and worthy of its own unique episodic processing. At the same time, completion of learned items in memory is in overdrive.

        The perceptual and memory systems of the human brain are complex and staged and often work in concert. By the time information is received by the entorhinal cortex from higher-order cortices or via visual processing routes, that information is already segmented to some extent and associated with unique neural representations (e.g., Kent, Hvoslef-Eide, Saksida, & Bussey, 2016). But the fine tuning necessary to make a memory of a particular event distinct from one in the previous year, or the previous day, or ten minutes ago, occurs as this information travels from the entorhinal cortex to the dentate gyrus where it becomes more sparsely distributed, before it is projected onto the CA3 (Rolls, 2016), primed and ready for pattern completion.

References

Ahn, J., & Lee, I. (2014). Intact CA3 in the hippocampus is only sufficient for contextual

behaviour based on well-learned and unaltered visual background. *Hippocampus, 24,*

1081–1093.

Bakker, A., Kirwan, C. B., Miller, M., & Stark, C. E. L. (2008). Pattern separation in the human

hippocampal CA3 and dentate gyrus. *Science, 319,* 1640–1642.

Barense, M. D., Henson, R. N. A., Lee, A. C. H., & Graham, K. S. (2010). Medial temporal lobe

activity during complex discrimination of faces, objects, and scenes: Effects of

viewpoint. *Hippocampus, 20,* 389–401.

Berron, D., Schütze, H., Maass, A., Cardenas-Blanco, A., Kuijf, H. J., Kumaran, D., & Düzel, E.

(2016). Strong evidence for pattern separation in human dentate gyrus. *Neuroscience, 36,*

7569–7579.

Besnard, A., & Sahay, A. (2016). Adult hippocampal neurogenesis, fear generalization, and

stress. *Neuropsychopharmacology, 41,* 24–44.

Blumenfeld, H. (2010). *Neuroanatomy through clinical cases* (2nd ed.). Sunderland, Mass.:

Sinauer Associates.

Chadwick, M. J., Bonnici, H. M., & Maguire, E. A. (2014). CA3 size predicts the precision of

memory recall. *Proceedings of the National Academy of Sciences of the United States of*

America, 111, 10720–10725.

Crawford, J. R., & Garthwaite, P. H. (2002). Investigation of the single case in neuropsychology:

Confidence limits on the abnormality of test scores and test score differences.

Neuropsychologia, 40, 1196–1208.

Crawford, J. R., & Garthwaite, P. H. (2005). Testing for suspected impairments and dissociations in single-case studies in neuropsychology: Evaluation of alternatives using Monte Carlo simulations and revised tests for dissociations. *Neuropsychology, 19,* 318–331.

Crawford, J. R., Garthwaite, P. H., & Slick, D. J. (2009). On percentile norms in neuropsychology: Proposed reporting standards and methods for quantifying the uncertainty over the percentile ranks of test scores. *The Clinical Neuropsychologist, 23*, 1173–1195.

Danielson, N. B., Kaifosh, P., Zaremba, J. D., Lovett-Barron, M., Tsai, J., Denny, C. A., Balough, E. M., Goldberg, A. R., Drew, L. J., Losonczy, A., Hen, R., & Kheirbek, M. A. (2016). Distinct contributions of adult-born hippocampal granule cells to memory encoding. *Neuron, 90,* 101–112.

Deuker, L., Doeller, C. F., Fell, J., & Axmacher, N. (2014). Human neuroimaging studies on the hippocampal CA3 region–integrating evidence for pattern separation and completion. *Frontiers in Cellular Neuroscience, 8,* 1–9

Duff, M. C., Warren, D. E., Gupta, R., Vidal, J. P. B., Tranel, D., & Cohen, N. J. (2012). Teasing apart tangrams: Testing hippocampal pattern separation with a collaborative referencing paradigm. *Hippocampus, 22,* 1087–1091.

Duvernoy, H. M. (2005). *The Human Hippocampus (3rd ed.).* Berlin: Springer-Verlag.

Farovik, A., Dupont, L. M., & Eichenbaum, H. (2010). Distinct roles for dorsal CA3 and CA1 in memory for sequential nonspatial events. *Learning & Memory, 17,* 12–17.

Gilbert, P. E., Holden, H. M., Sheppard, D. P., & Morris, A. M. (2016). Pattern separation: A key processing deficit associated with aging? In P. A. Jackson, A. A. Chiba, R. F. Berman, & Michael E. Ragozzino (Eds.), *The neurobiological basis of memory: A*

system, attribute, and process analysis (pp. 115-135). Springer International Publishing, Cham, Switzerland.

Gilbert, P. E., Kesner, R. P., & Lee, I. 2001. Dissociating hippocampal subregions: Double dissociation between dentate gyrus and CA1. *Hippocampus, 11,* 626–636.

Hollingworth, A., & Henderson, J. M. (1998). Does consistent scene context facilitate object perception? *The Journal of Experimental Psychology: General, 127,* 398–415.

Hunsaker, M. R., & Kesner, R. P. (2013). The operation of pattern separation and pattern completion processes associated with different attributes or domains of memory. *Neuroscience & Biobehavioral Reviews, 37,* 36–58

Johnston, S. T., Shtrahman, M., Parylak, S., Gonçalves, J. T., & Gage, F. H. (2016). Paradox of pattern separation and adult neurogenesis: A dual role for new neurons balancing memory resolution and robustness. *Neurobiology of Learning and Memory, 129*, 60–68.

Kent, B. A., Hvoslef-Eide, M., Saksida, L. M., & Bussey, T. J. (2016). The representational-hierarchical view of pattern separation: Not just hippocampus, not just space, not just memory? *Neurobiology of Learning and Memory, 129,* 99–106.

Kesner, R. P., Kirk, R. A., Yu, Z., Polansky, C., & Musso, N. D. (2016). Dentate gyrus supports slope recognition memory, shades of grey-context pattern separation and recognition memory, and ca3 supports pattern completion for object memory. *Neurobiology of Learning and Memory, 129,* 29–37.

Kirwan, B. C., Hartshorn, A., Stark, S. M., Goodrich-Hunsaker, N., Hopkins, R. O., Stark, C. E. L. (2012). Pattern separation deficits following damage to the hippocampus. *Neuropsychologia, 50,* 2408–2414.

Knowlton, B. J. & Eldridge, L. L. (2006). Mnemonic binding in the medial temporal lobe. In H. D. Zimmer, A. Mecklinger, & U. Lindenberger (Eds.), *Handbook of binding and memory: Perspectives from cognitive neurocoscience* (pp 93–526). Oxford University Press, Oxford, U.K.

Kwan, D., Craver, C. F., Green, L., Myerson, J., Gao, F., Black, S. E., and Rosenbaum, R. S. (2015). Cueing the personal future to reduce discounting in intertemporal choice: Is episodic prospection necessary? *Hippocampus, 25,* 432–443.

Lacy, J. W., Yassa, M. A., Stark S. M., Muftuler, L. T., and Stark, C. E. L. (2011). Distinct pattern separation related transfer functions in human CA3/dentate and CA1 revealed using high-resolution fMRI and variable mnemonic similarity. *Learning & Memory, 18,* 15–18.

Leranth, C., & Hajszan, T. (2007). Extrinsic afferent systems to the dentate gyrus. *Progress in Brain Research*, *163*, 63–799.

Leutgeb, J. K., & Leutgeb, S. (2014). The contribution of hippocampal subregions to memory coding. In M. S. Gazzaniga & G. R. Mangun (Eds.), *The cognitive neurosciences, 5th ed.,* (pp. 547–555). Cambridge, MA: MIT Press.

Leutgeb, J. K., Leutgeb, S., Moser, M.B., & Moser, E. I. (2007). Pattern separation in the dentate gyrus and CA3 of the hippocampus. *Science, 315,* 961–966.

Maguire, E. A., Gadian, D. G., Johnsrude, I. S., Good, C. D., Ashburner, J., Frackowiak, R. S. J., Frith, C. D. (2000). Navigation-related structural change in the hippocampi of taxi drivers. *Proceeding of the National Academy of Sciences of the United States of America, 97,* 4398–4403.

Marr, D. (1971). Simple memory: a theory for archicortex. *Philosophical Transactions of the Royal Society B: Biological Sciences, 262,* 23–81.

McHugh, T. J., Jones, M. W., Quinn, J. J., Balthasar, N., Coppari, R., Elmquist, J. K., Lowell, B. B., Fanselow, M. S., Wilson, M. A., & Tonegawa, S. (2007). Dentate gyrus NMDA receptors mediate rapid pattern separation in the hippocampal network. *Science, 317,* 94–99.

Molitor, R. J., Ko, P. C., Hussey, E. P., & Ally. B. A. (2014). Memory-related eye movements challenge behavioral measures of pattern completion and pattern separation. *Hippocampus, 24,* 666–672.

Mueller, S. G., & Weiner, M. W. (2009). Selective effect of age, apo e4, and alzheimer's disease on hippocampal subfields. *Hippocampus, 19,* 558–564.

Myers, C. E., & Scharfman, H. E. (2011). Pattern separation in the dentate gyrus: A role for the CA3 backprojection. *Hippocampus, 21,* 1190–1215.

Nakashiba, T., Cushman, J.D., Pelkey, K.A., Renaudineau, S., Buhl, D.L., McHugh, T.J., Rodriguez Barrera, V., Chittajallu, R., Iwamoto, K.S., McBain, C.J., et al. (2012). Young dentate granule cells mediate pattern separation, whereas old granule cells facilitate pattern completion. *Cell, 149,* 188–201.

Nakazawa, K., Quirk, M. C., Chitwood, R. A., Watanabe, M., Yeckel, M. F., Sun, L. D., Kato, A., Carr, C. A., Johnston, D., Wilson, M. A., & Tonegawa, S. (2002). Requirement for hippocampal CA3 NMDA receptors in associative memory recall. *Science, 297,* 211–218.

Neunuebel, J. P., & Knierim, J. J. (2014). CA3 retrieves coherent representations from degraded

    input: Direct evidence for CA3 pattern completion and dentate gyrus pattern separation.

    Neuron, 81, 416–427.

Newman, E. L., & Hasselmo, M. E. (2014). CA3 sees the big picture while dentate gyrus splits

    hairs. *Neuron, 81,* 226–228.

Norman, K. A., Detre, G., & Polyn, S. M. (2008). Computational models of episodic memory. In

    R. Sun (Ed.), *The cambridge handbook of computational psychology* (pp. 189–225). New

    York: Cambridge University Press.

O'Reilly, R. C., & McClelland, J. L. (1994). Hippocampal conjunctive encoding, storage, and

    recall: Avoiding a trade-off. *Hippocampus, 4,* 661–682.

Rempel-Clower, N., Zola, S. M., Squire, L. R., & Amaral, D. G. (1996). Three cases of enduring

    memory impairment after bilateral damage limited to the hippocampal formation. *The*

    Journal of Neuroscience, 16, 5233–5255.

Robertson, L. C., Knight, R. T., Rafal, R., & Shimamura, A. P. (1993). Cognitive

    neuropsychology is more than single-case studies. *Journal of Experimental Psychology:*

    Learning, Memory, and Cognition, 19, 710–717.

Rolls, E. T. (2016). Pattern separation, completion, and categorisation in the hippocampus and

    neocortex. *Neurobiology of Learning and Memory, 129,* 4–128.

Rosenbaum, R. S., Gilboa, A., & Moscovitch, M. (2014). Case studies continue to illuminate the

    cognitive neuroscience of memory. *Annals of the New York Academy of Sciences, 1316*,

    105–133.

Santoro, A. (2013). Reassessing pattern separation in the dentate gyrus. *Frontiers in Behavioral*

    Neuroscience, 7, 1–4.

Schmidt, B., Marrone, D. F., & Markus, E. J. (2012). Disambiguating the similar: The dentate gyrus and pattern separation. *Behavioural Brain Research, 226,* 56–65.

Stark, S. M., Stevenson, R., Wu, C., Rutledge, S., & Stark, C. E. L. (2015). Stability of age-related deficits in the mnemonic similarity task across task variations. *Behavioral Neuroscience, 1*29, 257–268.

Stark, S. M., Yassa, M. A., Lacy, J. W., & Stark, C. E. L. (2013). A task to assess behavioral pattern separation (BPS) in humans: Data from healthy aging and mild cognitive impairment. *Neuropsychologia, 51,* 2442–2449.

Suzuki, W. L., & Amaral, D. G. (1994). Perirhinal and parahippocampal cortices of the macaque monkey: cortical afferents. *Journal of comparative neurology, 350,* 497−533.

Tompary, A., Duncan, K., & Davachi, L. (2016). High-resolution investigation of memory-specific reinstatement in the hippocampus and perirhinal cortex. *Hippocampus.* Advance online publication, doi:http://dx.doi.org/10.1002/hipo.22582.

Treves, A., & Rolls, E. T. (1994). A computational analysis of the role of the hippocampus in memory. *Hippocampus 4,* 374–391.

Tulving, E. (2000). Chronesthesia: Conscious Awareness of Subjective Time. In D. T. Stuss, & R. T. Knight (Eds.), *Principles of frontal lobe function*, 311–325. New York: Oxford University Press.

Ungerleider, L. G., & Mishkin, M. (1982). Two cortical visual systems. In D. J. Ingle, R. J. W. Mansfield, & M. S. Goodale (Eds.), *The analysis of visual behavior* (pp. 549–586). Cambridge, MA: MIT Press.

Ungerleider, L. G., & Pasternak, T. (2004). Ventral and dorsal processing streams. In L. M. Chalupa & J. S. Werner (Eds.), *The visual neurosciences* (pp. 541–562). Cambridge, MA: MIT Press.

Vieweg, P., Stangl, M., Howard, L. R., & Wolbers, T. (2015). Changes in pattern completion — a key mechanism to explain age-related recognition memory deficits? *Cortex, 64,* 343–351.

Wang, Z., Neylan, T. C., Mueller, S. G., Lenoci, M., Truran, D., Marmar, C. R., . . . Schuff, N. (2010). Magnetic resonance imaging of hippocampal subfields in posttraumatic stress disorder. *Archives of General Psychiatry, 67,* 296-303.

Weeden, C. S. S., Hu, N. J., Ho, L. U. N., & Kesner, R. P. (2014). The role of the ventral dentate gyrus in olfactory pattern separation. *Hippocampus, 24,* 553–559.

Wilson, I. A., Gallagher, M., Eichenbaum, H., & Tanila, H. (2006). Neurocognitive aging: Prior memories hinder new hippocampal encoding. *Trends in Neurosciences, 29,* 662–670.

Wilson, I. A., Ikonen, S., Gureviciene, I., McMahan, R. W., Gallagher, M., Eichenbaum, H., & Tanila, H. (2004). Cognitive aging and the hippocampus: How old rats represent new environments. *The Journal of Neuroscience, 24,* 3870–3878.

Witter, M. P. (2007). The perforant path: projections from the entorhinal cortex to the dentate gyrus. *Progress in Brain Research, 163,* 43–61.

Yassa, M. A., Lacy, J. W., Stark, S. M., Albert, M. S., Gallagher, M., & Stark, C. E. L. (2011). Pattern separation deficits associated with increased hippocampal CA3 and dentate gyrus activity in nondemented older adults. *Hippocampus, 21,* 968–979.

Yushkevich, P. A., Pluta, J. B., Wang, H., Xie, L., Ding, S. L., Gertje, E. C., Mancuso, L., Kliot, D., Das, S. R., & Wolk, D. A. (2015). Automated volumetry and regional thickness

analysis of hippocampal subfields and medial temporal cortical structures in mild

cognitive impairment. *Human Brain Mapping, 36,* 258–287.

Zola-Morgan, S. M., Squire, L. R., & Amaral, D. G. (1986). Human amnesia and the medial

temporal region: enduring memory impairment following a bilateral lesion limited to

field CA1 of the hippocampus. *The Journal of Neuroscience. 6*, 2950–2967.

Table 1

BL's Percentage Volume of Parietal, Occipital and Temporal Lobe Structures Relative to Means

of Eight Healthy Controls[a]

	IOG	LOTG	LG	AG	SMG	SPL	Pre	ITG	PHG
Left hemisphere	85%	91%	111%	111%	74%	73%	82%	112%	100%
p[b]	0.58	0.58	0.64	0.25	0.07	**0.02**	0.06	0.24	0.98
Right hemisphere	94%	99%	97%	111%	96%	85%	74%	99%	93%
p[b]	0.84	0.97	0.78	0.35	0.82	0.27	**0.05**	0.96	0.76

Table 1 notes. IOG, Inferior Occipital Gyrus; LOTG, Lateral Occipito-Temporal Gyrus; LG,

lingual gyrus; AG, angular gyrus; SMG, supramarginal gyrus; SPL, superior parietal lobule; Pre,

precuneus; ITG, inferior temporal gyrus; PHG, parahippocampal gyrus.

[a] Volumes normalized by intracranial volume, whereby each participant's raw grey matter

volume was divided by estimated total intracranial volume (eTIV).

[b] Using statistical methods tailored to single case experiments (Crawford & Garthwaite, 2002).

Bolded p values ≤ 0.05.

Table 2

BL's Neuropsychological Data

			WMS-R/III/IV		Verb Learn.		ROCF		
FSIQ	WCST	LF	LP/M-I	LP/M-II	AQ	LDFC	R	C	DR
92	6	11	8	6	8	7	10	6	5

Table 2 notes. FSIQ: Wechsler Abbreviated Scale of Intelligence–IV. WCST: Wisconsin Card Sorting Test, number of completed categories /6. The following measures are reported in scaled scores: LF: letter fluency. Verb Learn: Verbal learning based on California Verbal Learning Test-II; AQ, acquisition; LDFR, long delay free recall; R, recognition. ROCF: Rey-Osterrieth Complex Figure, C, copy, DR, delayed recall. BL's relative weakness within the visuospatial domain on the copy condition of ROCF may relate to volume loss within superior-posterior parietal cortex (see Table 2). It is unlikely that this deficit and volume loss explain performance on tests of discrimination and completion (Vieweg et al., 2015; Zola-Morgan et al., 1986). Moreover, regions of inferotemporal cortex known to be involved in object recognition remain structurally intact.

Figure Captions

Figure 1. Hippocampal formation. Figure adapted from from *The Human Hippocampus (3rd ed.),* H. Duvernoy et al., p. 18, Copyright (2005), with permission from Springer.

Figure 2. Left: forward and back projections in the entorhinal cortex and hippocampal formation. Right: Detailed representation of excitatory neurons within the trisynaptic circuit. Figure reprinted from *Neurobiology of Learning and Memory, 129,* Edmund T. Rolls, Pattern separation, completion, and categorisation in the hippocampus and neocortex, 4–28, Copyright (2016), with permission from Elsevier. Figure Abbreviations. "D: Deep pyramidal cells. DG: Dentate Granule cells. F: Forward inputs to areas of the association cortex from preceding cortical areas in the hierarchy. mf: mossy fibers. PHG: parahippocampal gyrus and perirhinal cortex. pp: perforant path. rc: recurrent collateral of the CA3 hippocampal pyramidal cells. S: Superficial pyramidal cells. 2: pyramidal cells in layer 2 of the entorhinal cortex. 3: pyramidal cells in layer 3 of the entorhinal cortex. The thick lines above the cell bodies represent the dendrites." (Rolls, 2016, p. 6).

Figure 3. Connections from three different sources onto each rat CA3 cell. Figure reprinted from *Neurobiology of Learning and Memory, 129,* Edmund T. Rolls, Pattern separation, completion, and categorisation in the hippocampus and neocortex, 4–28, Copyright (2016), with permission from Elsevier.

Figure 4. Hippocampal segmentation of BL and age-matched control. Legend: Red (CA3&DG); Green (CA1-2 transition); Yellow (CA1); Blue (subiculum).

Figure 5. MRI scans of BL's hippocampus revealing highly selective lesions to the dentate gyrus. Notes. (A) Reference image, adapted from Duvernoy (2005), illustrates normal anatomy of the left hippocampus. The hippocampal strata (SRLM) lie along the interface between the

dentate gyrus and CA1-CA3 subfields and subiculum. The SRLM is exposed as a band of hyperintensity on the inverted coronal T2-weighted hippocampal images as seen in B, and is a landmark to define the area of dentate gyrus. (B) The inverted T2 through the middle body of BL's hippocampus shows a hypointense lesion (hyperintense in non-inverted T2) almost exclusively affecting dentate gyrus. (C) T2 of the sagittal view depicts the length of the hippocampal lesion, which extends across almost the entire dentate gyrus in both hemispheres (arrows).

Figure 6. MST paradigm. Figure reprinted *from Neuropsychologia, 51* (12), Shauna M. Stark, Michael A. Yassa, Joyce W. Lacy, Craig E. L. Stark, A task to assess behavioral pattern separation (BPS) in humans: Data from healthy aging and mild cognitive impairment, 2442– 2449, Copyright (2013), with permission from Elsevier.

Figure 7. MIC stimuli. Notes: (A) At study, participants learn to identify five different line drawings (targets): bar, bedroom, dining room, kitchen and library, shown at 100%. (B) At test, targets and new images (foils) were presented for 2 sec each in varying degrees of stimuli completeness.

Figure 8. MST: Recognition accuracy, % correct (±SEM controls). Significant differences between controls and BL are indicated with * for *p* <.05,

Figure 9. MIC task. Notes: (A) At study, participants learned to identify five different line drawings (targets): bar, bedroom, dining room, kitchen and library (shown). At test, targets and foils, e.g., office (shown), were presented in varying degrees of stimuli completeness; 35% shown for library at left and office at right. (B) Recognition accuracy, mean % correct (± SEM controls), for targets (learned items) at 100% and the four masked completeness levels. (C) Recognition accuracy, mean % correct (± SEM controls), for foils (new items) at 100% and the

four masked completeness levels. (D) MIC bias scores (targets minus foils) at each level of

completeness (± SEM controls). Significant differences between controls and BL are indicated

with * separately for each level of stimuli completeness.

Figure 10. MST and MIC dissociation. Notes: Bias percentages for the MST (i.e., the LDI score)

and the MIC (degraded, or masked images only). Data are represented as mean bias score ± SEM

for controls. Significant differences between controls and BL are indicated with * for $p < .05$, **

for $p < .01$ and *** for $p < .001$.
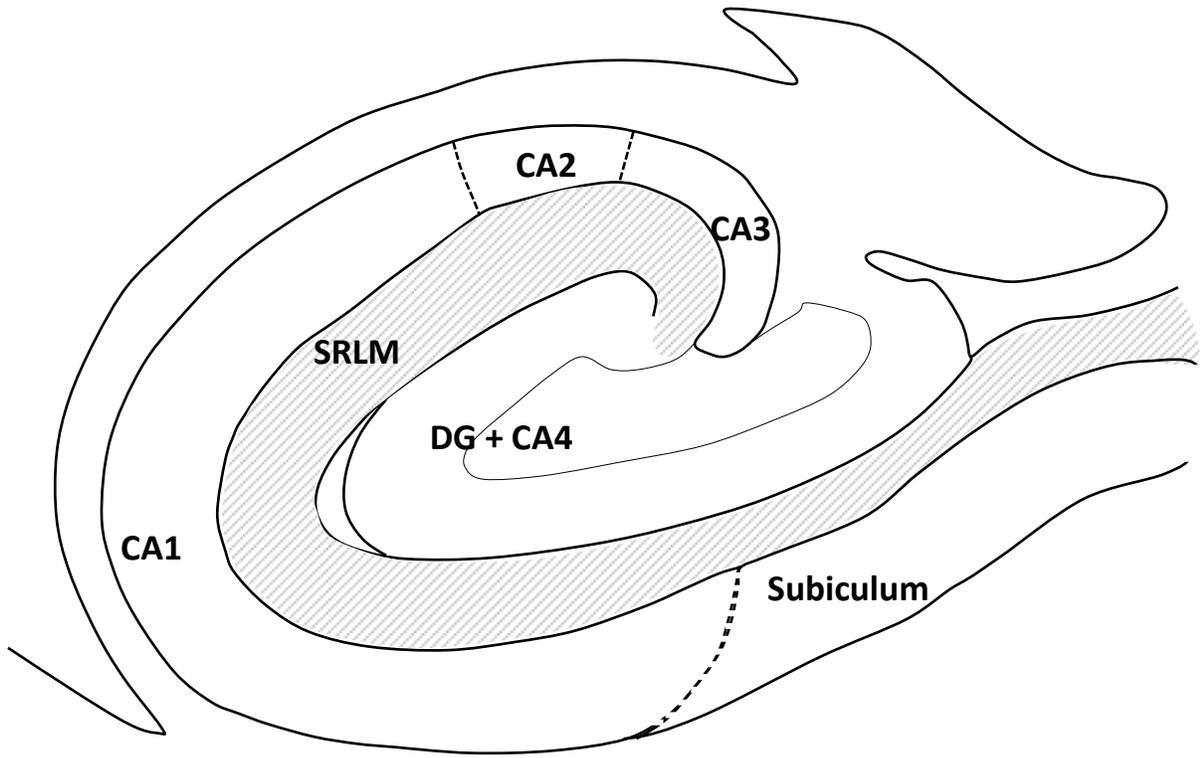
Figure 1.
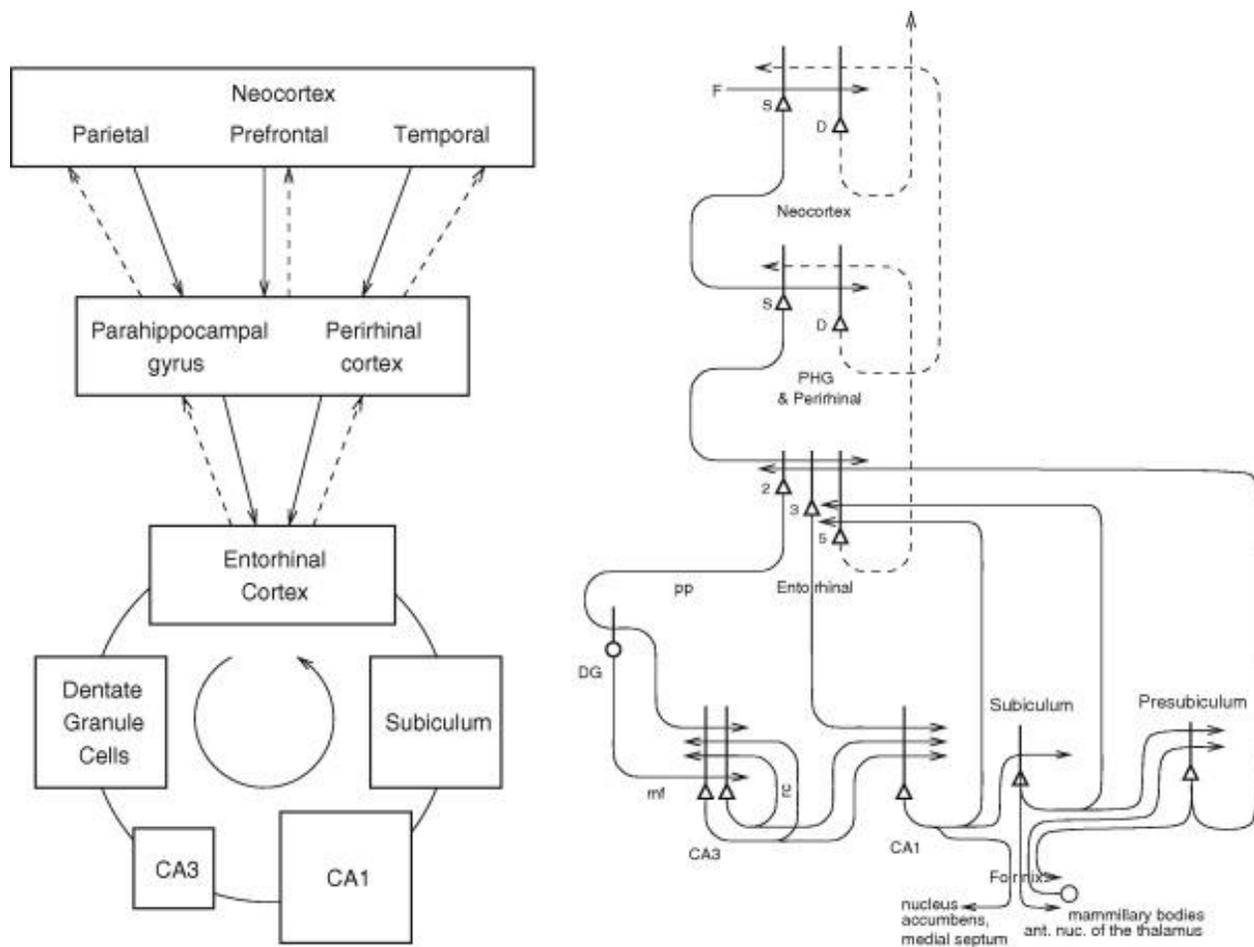
Figure 2.
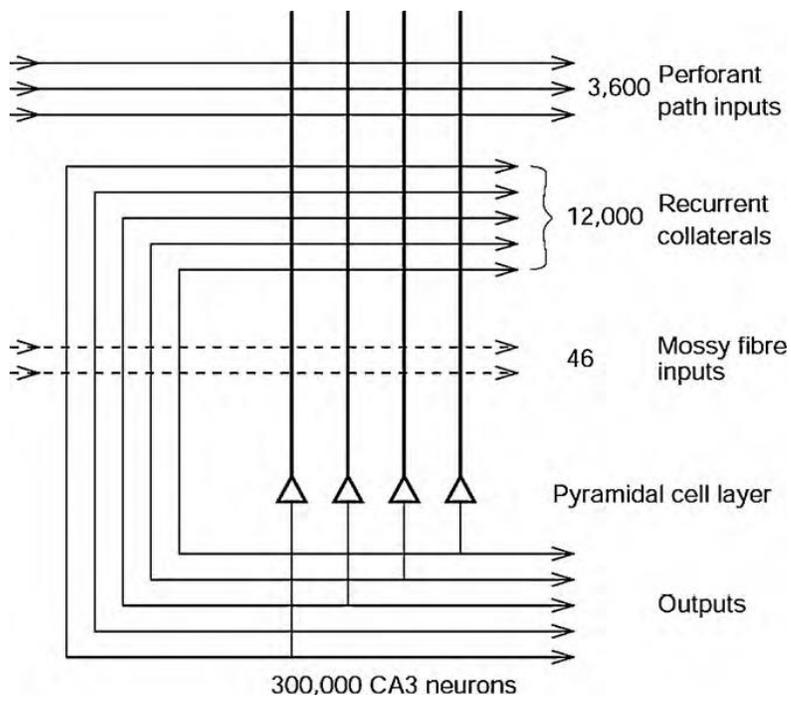
Figure 3.
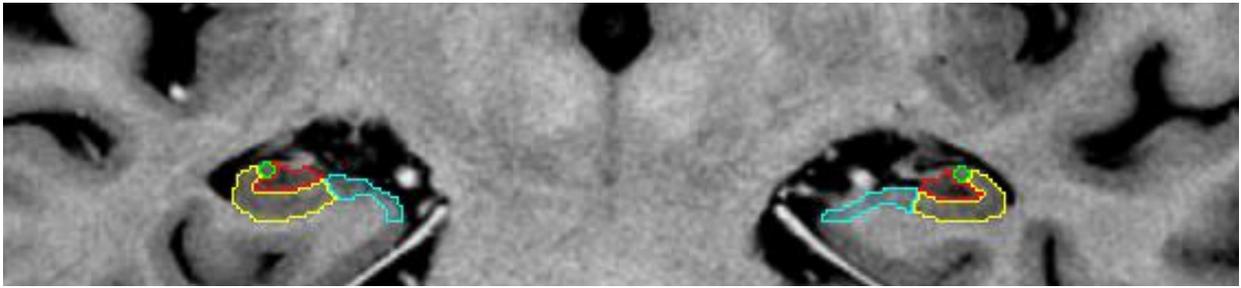
A) BL (above)
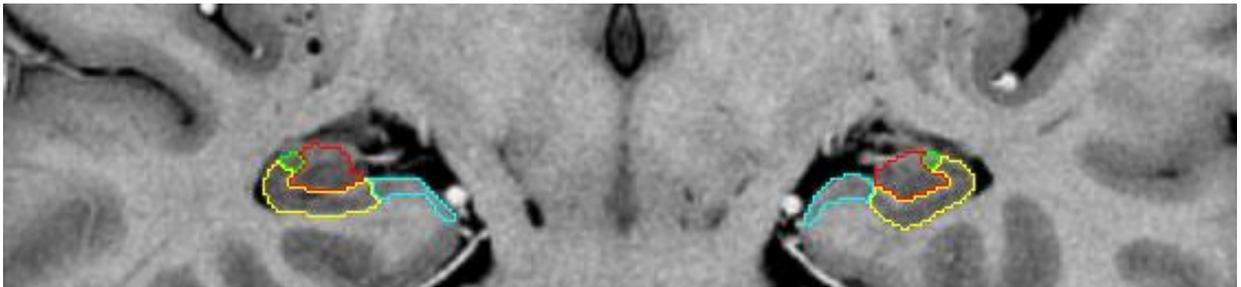
B) Age-matched control (above)

Figure 4.
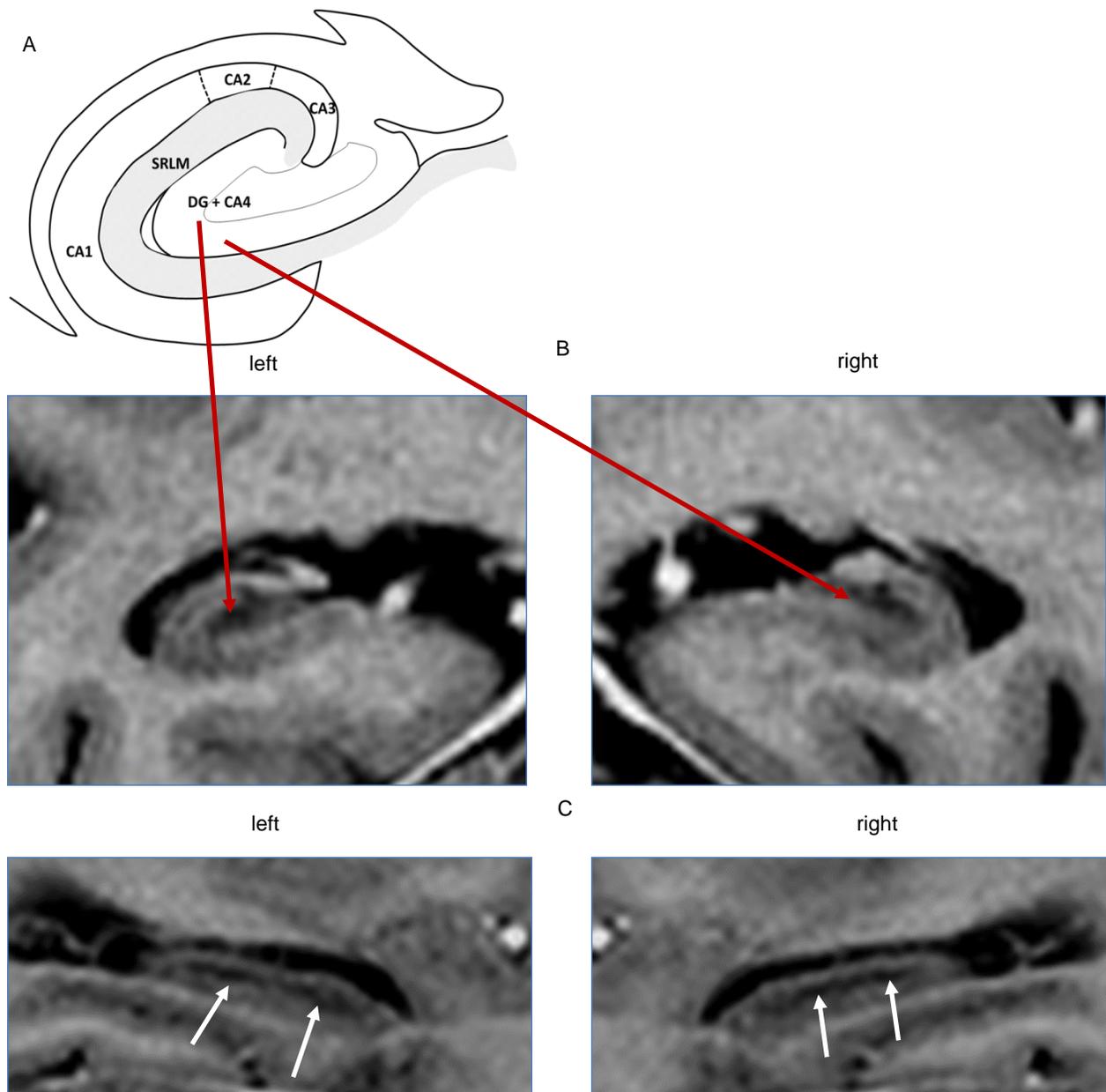
Figure 5.
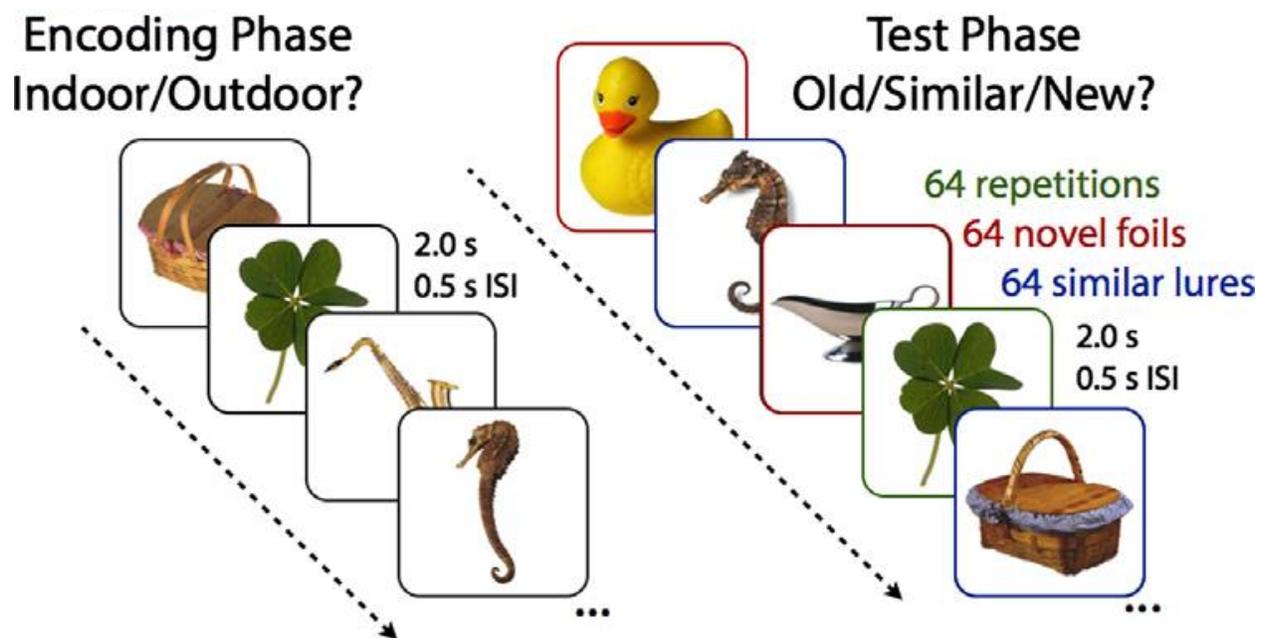
Figure 6.

A.


B.
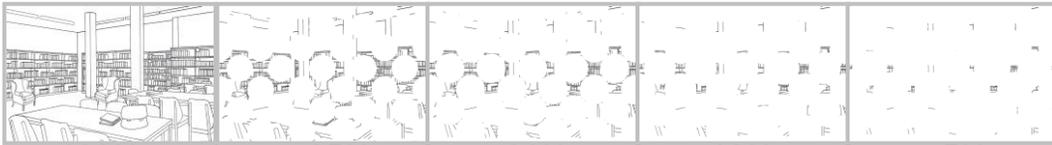
100%   **35%**   **21%**   **12%**   **5%**

% completeness

Figure 7.
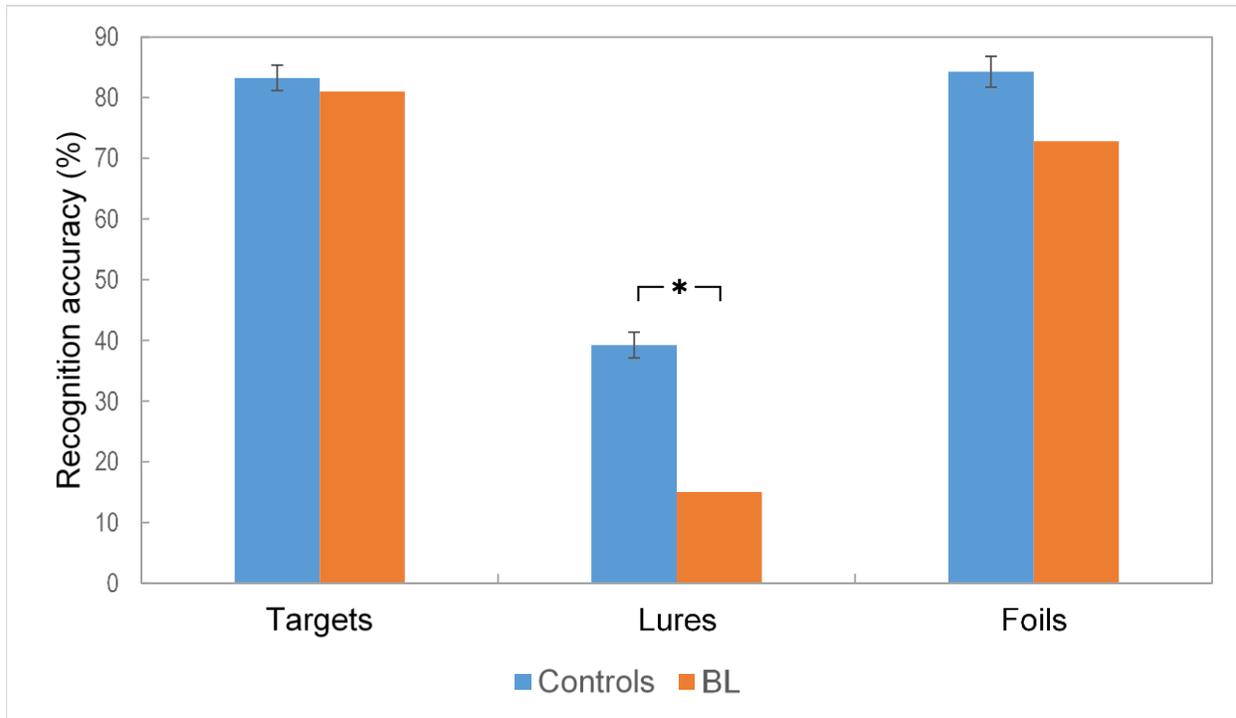
Figure 8.

Figure 9.

Figure 10.